A unified mechanical based approach to fracture properties estimates of rubbers subjected to aging

R. Kadri [a,b,c], M. Nait Abdelaziz [a,*], B. Fayolle [c], M. Ben Hassine [b], J.F. Witz [d]

[a] Université de Lille, UML – Unité de Mécanique de Lille – J. Boussinesq, ULR 7512, 59650 Villeneuve d'Ascq, France
[b] Département MMC, EDF Lab, F-77818 Moret-sur-Loing, France
[c] Laboratoire des Procédés et Ingénierie en Mécanique et Matériaux (PIMM), UMR CNRS 8006, Arts et Métiers ParisTech, F-75013 Paris, France
[d] Université de Lille, LamCube – UMR 9013, 59650 Villeneuve d'Ascq, France

A B S T R A C T

In this work, the influence of aging on the mechanical properties at break of rubber materials are examined. When subjected to physical-chemical aging, the structure of the rubber network is deeply modified through two main mechanisms: crosslinking and chain scission. These aging mechanisms act both on the mechanical behaviour and on the fracture properties of the rubber materials.

The goal of this work is to propose a predictive mechanical tool able to give estimates of these mechanical properties. To address this issue, an hyperelastic constitutive model based upon the energy limiter approach, was coupled with physical-chemical parameters in order to capture the whole mechanical behaviour of the damaged materials beyond the fracture. That allows fracture stress and strain estimates.

A wide set of materials and experimental data extracted from the literature or obtained in our team were selected based upon the aging mechanism they can exhibit.

We found that the elastically active chains concentrations and the swelling rate can be used as relevant in-dicators of damage either for crosslinking or chain scission process.

These parameters are then introduced as damage parameters in the mechanical modelling. The proposed approach leads to very satisfactory predictions, either to capture the whole mechanical behaviour in uniaxial tension or in terms of stress and strain at break estimates.

1. Introduction

Because of the wide set of properties that elastomers can exhibit, such as especially their ability to withstand very large reversible deformations, the use of rubber materials is considerably widespread in many industrial applications, including air and ground transportation, energy and health. Without being exhaustive, anti-vibration systems, gaskets, electrical insulation, tires, medical prostheses are just a few examples of the use of these materials.

Elastomers are generally classified as amorphous polymers, constituted of long linear macromolecular chains, linked together by chemical bridges (most often sulphur or peroxide bonds) also called crosslinking nodes. The typical behaviour of elastomers is due to their glass transition temperature T_g which is much lower than their operating temperature (generally the ambient temperature), and therefore facilitates the mobility of macromolecular chains.

Depending on the operating conditions, the material interacts with its environment and can undergo complex mechanical loading combined with severe conditions of temperature and humidity. In some cases, they can also be subjected to UV (open air applications) or gamma radiations (nuclear power plant…). That generally leads to slow and irreversible evolution of the structure, which influence the mechanical behaviour and the ultimate properties of the elastomer such as stress or strain at break. This evolutionary process is generally referred to as aging, which includes many sources, both physical–chemical and mechanical. The issue to be addressed is therefore the prediction of the operating life of the rubber components which must be assessed during the design process.

Our general purpose is to assess the validity of the coupled approaches used to predict fracture and this work especially focuses on the energy limiter approach. This novel approach, developed in the thermodynamics framework, allows to capture the whole behaviour of the material, up to and beyond the fracture. Because equations are derived

from the expression of a free energy, it also accounts for multiaxial loading paths, allowing the derivation of stress and strain components.

Indeed, Nait Abdelaziz et al. (2019) has shown the advantages of this approach when dealing with EPDM exhibiting crosslinking mechanism during thermo-oxidative aging. This work aims to extend this approach to rubber materials whatever the degradation mode or predominant degradation mechanism in the network during aging (crosslinking or chain scission).

In the case of crosslinking, the molar mass between crosslinks (M_c) seems to be the relevant indicator of the macromolecular network degradation and can be associated to failure properties, especially elongation at break (Wall and Flory, 1951) or toughness expressed as (Lake, 2003):

$$G_0 = K.M_c^{\frac{1}{2}} \quad (1)$$

This theory has been successfully applied for many cases where crosslinking is predominant. However, in the case of chain scission, the relevance of this indicator for describing the material degradation is questionable because the physical meaning of M_c is lost since chain scission mechanism leads to occurrence of dangling chains or free chains not attached to the network. Generally, chain scission leads to increase statistically M_c mean value and thus to increase the failure properties predicted by the previous theory which is contradictory with the experimental observations in the literature (Le Gac et al., 2014).

The main idea which has to be assessed is to explore the evolution of the macromolecular network through two parameters: the concentration of elastically active chains (EAC) ν, and the swelling ratio Q, as generalized parameters able to report the whole behaviour and failure properties.

To achieve these objectives, we will rely on many sets of experimental data. Because in our own data only crosslinking is observed, an effort has been made to select data exhibiting chain scission in the literature.

This paper is therefore organized as follows:

A literature review is first presented including both chemical and mechanical degradation due to aging. The energy limiter approach which is used to capture the whole mechanical behaviour including the fracture process is then detailed. The third section present the studied materials and experimental procedures. The fourth section is devoted to the description of the network degradation of the studied materials allowing highlighting the relevant chemical-physical parameters to be introduced in the mechanical modelling. In the fifth section, the capabilities of the modelling are then discussed. Finally, some concluding remarks are given.

2. Literature review

The combination of physical and chemical changes in the macromolecular network over time is generally responsible for the aging of elastomers (Ehrenstein and Pongratz, 2007). Various works (Bolland and Gee, 1946; Decker et al., 1973; Rincon-Rubio et al., 2001; Tobolsky et al., 1950) have allowed highlighting the chemical mechanisms of radio-oxidation and thermo-oxidation of elastomers. They have demonstrated that these transformations of the macromolecular network are generated through two mechanisms, which are crosslinking and chain scission, these mechanisms inducing a degradation of the mechanical properties (Belbachir et al., 2010; M. Ben Hassine et al., 2014; De Almeida, 2014; Planes et al., 2010a; Planes et al., 2010b; Planes et al., 2009; Shabani, 2013; Sidi, 2016).

Nevertheless, in some cases, the two mechanisms can be pointed out. For example, it has been observed in some EPDM materials cross-linked with peroxide, a crosslinking mechanism at the early stage of aging which is progressively followed by a chain scission mechanism as the exposure time increases (Planes et al., 2010a; Planes et al., 2010b; Planes et al., 2009).

For EPDM, this early-stage crosslinking is attributed to the presence of ENB residues in the matrix. Indeed, the initial crosslinking density first depends on the ENB content fraction but also PE/PP ratio, increasing PE content leading to an increase of the crosslink density. Thus, the maximum chemical crosslink density that the material could reach during aging depends both on the ENB content of the EPDM and on the crosslinks possibly formed via the PE units during the material manufacturing (De Almeida, 2014; Planes et al., 2009).

In the case of a cross-linked EPDM matrix, filled with 150phr of ATH micrometric particles, Gabrielle et al. (2011) compared the material degradation of the filled material to that of the pure matrix. NMR (nuclear magnetic resonance spectroscopy) measurements were achieved on the materials at a solid state and the evolutions of the transverse relaxations H during the thermo-oxidation were analysed. They show a very significant increase of both the dangling chains fraction and of the soluble fraction for the filled EPDM after 5 days' exposure at 80 °C, while no modification of the pure EPDM network was pointed out. The observed differences between the unfilled and filled matrix is attributed to the presence of the filler particles.

In his work, Pubellier (2017) has investigated the influence of the ATH filler on the evolution of the macromolecular network during thermo-oxidation. The studied material is also an EPDM rubber filled with 100phr of ATH. Once again, the filled material exhibits an early-stage degradation compared to the pure matrix. According to the author, the chain scission in the composite material (filled EPDM) begin in the vicinity of the fillers and then spreads around into the matrix. This degradation rate increase is attributed to a specific hydroperoxide species decomposition generated during thermo-oxidation close to the surface of the fillers, consequently shortening the oxidation induction period of the composite compared to that of the pure matrix.

Concerning the mechanical behaviour of elastomers, hyperelasticity is the framework from which constitutive laws are generally derived. An increasing interest of researchers and engineers in the development of mechanical models able to fit the typical behaviour of such materials has been shown since 1940. Two general ways are adopted to deal with this kind of mechanical modelling: the so-called phenomenological models -see following reviews (Marckmann and Verron, 2006; Seibert and Schöche, 2000)- which aim at the faithful capture of the experimental results, and the micromechanical models, which are mostly based upon the statistical physics of polymer chains and networks –see the following reference (Heinrich et al., 1988). For both of them, a strain energy density function, from which strains and stresses are derived is postulated. According to that, the material can deform infinitely and therefore fracture is not accounted for in such modelling.

In general, fracture of rubbers is tackled by using own uncoupled or weakly coupled criteria with the constitutive law (Hamdi et al., 2006, 2007; Naït-Abdelaziz et al., 2012). Among these fracture criteria, Naït-Abdelaziz et al. (2012) used the intrinsic defect concept and derived a fracture criteria coupled with fracture mechanics. This approach was successfully applied to predict fracture of rubbers under multiaxial loadings (Ayoub et al., 2011; Ayoub et al., 2014; Naït-Abdelaziz et al., 2012) and to estimate the strain at break of an EPDM subjected to thermal aging conditions (Ben Hassine et al., 2014).

Dealing with the prediction of the long-term mechanical behaviour of EPDM rubbers in a thermo-oxidative environment, Colin et al (Colin et al., 2019) proposed a chemo-mechanical model which consists in two steps modelling. First, at the chemical level, the degradation kinetics of the macromolecular network is summarized through a mechanistic diagram made up of 19 elementary reactions describing the thermal oxidation of EPDM chains, allowing estimates of microstructural parameters such as the molar mass between crosslinks (M_c). These data are introduced in a second step, as an input parameter at the mechanical level to predict mechanical properties at break by using the stress limiter approach (Nait Abdelaziz et al., 2019).

As previously underlined, even these approaches can exhibit a weak coupling between the mechanical constitutive law and the fracture criteria, the equations are generally developed in the case of uniaxial tension. It then seems interesting to move towards modelling using a

strong coupling in one hand, and which can be generalized to three-dimensional cases, in another hand.

This is the way adopted by Volokh (2007) and Dal and Kaliske (2009) who have opened very interesting and different alternatives to address the issue of the coupling between the mechanical behaviour and the fracture.

Indeed, Dal and Kaliske (2009) have proposed a micromechanical approach to model the rupture of rubber. This approach starts from the description of a single chain which is modelled with a series construction of two springs, one being of the Langevin type representing the energy storage due to conformational changes induced by the deformation, and the second representing the energy stored in the polymer chain due to the interatomic displacement. The interatomic bond energy is described by using the Morse potential which governs the breaking of the polymer chain. The micro–macro scale transition is then achieved by using the micro-sphere model (Miehe, 2004; Miehe and Göktepe, 2005). This approach was successfully applied to some failure data in monotonic uniaxial tension, pure shear and equibiaxial tension tests.

From his side, Volokh (2007) has developed a macroscopic approach integrating directly the fracture process in the strain energy density function. The premise is relatively simple: a material cannot absorb an unlimited amount of energy, which is the flaw of all hyperelastic models. He suggested limiting this energy, using a parameter depending on the material and called the strain energy limiter. Many examples of application have been provided by the author, demonstrating the capabilities of this approach (Trapper and Volokh, 2010; Volokh, 2007; Volokh, 2010, 2013, 2017). Moreover, this approach have been successfully used by Nait Abdelaziz et al. (2019) to predict the influence of thermal oxidative aging on the ultimate mechanical properties of rubbers. The different works dealing with the influence of aging on the ultimate properties which were achieved on rubber materials (Ben Hassine et al., 2014; Colin et al., 2019; Nait Abdelaziz et al., 2019) have shown that, in the case of crosslinking mechanism, the molar mass between crosslinks is the relevant chemical parameter allowing describing the material degradation. The main equations of the energy limiter theory are summarized below.

3. Energy limiter approach

The development of constitutive laws for rubber materials are based upon the mechanics of continuous media and the thermodynamics framework under the assumption of finite strain. Hyperelasticity is the general framework which is used to build constitutive models allowing the derivation of stresses and strains for such materials (Bouaziz et al., 2019; Rosendahl et al., 2019; Zhong et al., 2019). It postulates the existence of a strain energy density function W which corresponds to the Helmholtz free energy ψ. In this case, the strain energy density is not thresholded and grows up to the infinite when increasing the deformation:

$$\begin{cases} \psi = W \\ \boldsymbol{F}\to\infty \Rightarrow \psi\to\infty \end{cases} \tag{2}$$

In eq. (2), $\boldsymbol{F}$ is the deformation gradient tensor.

To predict failure, Volokh (2007) proposed to bound the maximum energy that the material can absorb by integrating a material dependent constant φ, called material failure energy, and verifying the following condition.

$$\boldsymbol{F}\to\infty \Rightarrow \psi(W(\boldsymbol{F})) = \varphi \tag{3}$$

An expression of the free energy ψ has been therefore developed which follows the energy limit given by eq. (3). This development leads to the following new "free energy":

$$\psi(W) = \varphi - \varphi exp\left(-\frac{W}{\varphi}\right) \tag{4}$$

According to Volokh (2007), eq. (4) allows to describe the mechanical behaviour beyond the fracture initiation of soft materials, such as biological tissues, which exhibit a progressive rupture, and which is reflected on the stress–strain curve by a soft and continuous decreasing of the stress. Such an evolution law is not able to describe the sudden drop accompanying the failure of rubber materials. To address this issue, Volokh (2010) has proposed an alternative formulation of the free energy:

$$\psi = \frac{\varphi}{m}\left\{\Gamma\left(\frac{1}{m},0\right) - \Gamma\left(\frac{1}{m},\frac{W^m}{\varphi^m}\right)\right\} \tag{5}$$

where Γ is the upper gamma function $\Gamma(s,x) = \int_x^\infty t^{s-1}exp(-t)dt$ and m a material parameter controlling the slope of the stress drop.

The Cauchy stresses tensor takes the following form:

$$\boldsymbol{\sigma} = 2J^{-1}\boldsymbol{F}\frac{\partial\psi}{\partial\boldsymbol{C}}\boldsymbol{F}^T \tag{6}$$

where $\boldsymbol{C}$ is the right Cauchy-Green deformation tensor expressed as:

$$\boldsymbol{C} = \boldsymbol{F}^T\boldsymbol{F} \tag{7}$$

Knowing that $\frac{\partial\psi}{\partial W} = exp\left(-\frac{W^m}{\varphi^m}\right)$, the Cauchy stress tensor can be re-expressed as:

$$\boldsymbol{\sigma} = 2J^{-1}\boldsymbol{F}\frac{\partial W}{\partial\boldsymbol{C}}\boldsymbol{F}^T exp\left(-\frac{W^m}{\varphi^m}\right) \tag{8}$$

If taking the Arruda and Boyce (1993) model for the SED function W:

$$W = \nu RT N\left[\sqrt{\frac{I_1}{3N}}\beta + ln\left(\frac{\beta}{sinh\beta}\right)\right] \quad \text{with} \quad \beta = \mathscr{L}^{-1}\left(\sqrt{\frac{I_1}{3N}}\right) \tag{9}$$

And in the case of uniaxial tension, using the Cohen (1991) approximation, the Cauchy stress is reduced to the following expression:

$$\sigma = \frac{\nu RT}{3}\left(\frac{9N - I_1}{3N - I_1}\right)(\lambda^2 - \lambda^{-1})exp\left(-\frac{W^m}{\varphi^m}\right) \tag{10}$$

where R is the gas constant (8.314 J.K^{-1}.mol^{-1}), T the absolute temperature, ν the EAC concentration, N the number of Kuhn segments in the chain and λ is the stretch (maximum eigen value of $\boldsymbol{F}$).

Fig. 1 shows the comparison between the uniaxial tensile response of an unaged EPDM (EPDM-01), and the model, with $\nu = 10^{-3}$ mol/cm^3, $N = 21$ and $\varphi = 18.45$ MPa. A satisfactory agreement is highlighted, confirming the robustness of the energy limiter approach.

The influence of the parameter m is also depicted in Fig. 1. The lower the value of m the softener the stress drop. Consequently, a value of 100 for this parameter was chosen for all the calculations involved in this work.

Our purpose is therefore coupling the model parameters (ν and φ) to the network evolution during aging in order to predict as well the mechanical behaviour as the fracture properties such as the stress and strain at break. Moreover, the challenge is also to get these parameters from physical-chemical measurements.

4. Experimental

4.1. Materials

Because our goal was to extend the mechanical approach to materials exhibiting chain scission mechanisms, we focused on:

- EPDM-01: manufactured by a company, crosslinking mechanism;
- EPDM-02, EPDM-03: manufactured in a university lab, chain scission mechanism;
- PU, SR: manufactured by a company, chain scission mechanism.

Table 1 specifies the available data and that computed in this work. The EPDM-01 are issued from internal work of our group, while EPDM-02 and EPDM-03 materials data were extracted from the investigation of

A. De Almeida (De Almeida, 2014), PU (polyurethane) material data come from the work of Le Gac et al. (2013) and SR (silicone rubber) material data are the results of the research work of Kashi et al. (2018). For each material, different data are available in terms of figures that we have digitized.

Note that EPDM-01, PU and SR materials are commercial materials, therefore their formulations are not known or are not clearly defined.

In general, the numerical data were obtained by digitizing the results given in the form of plots, as reported in Table 2:

4.2. Aging

EPDM-01 samples were aged at 90, 110, 130 and 150 °C in air-ventilated ovens, ensuring air flow inside the oven during the thermo-oxidative aging process. After different exposure times, samples were taken from the oven and cooled at room temperature.

EPDM-02 and EPDM-03 materials (De Almeida, 2014) were exposed to γ radiations by using ^{60}Co sources. The irradiation process was carried out under an average dose rate of 1.3 kGy/h and at room temperature of about 20 °C, to reach total absorbed doses of 50, 120, 210, 250, 320, 350, 450, 600, 800 and 1000 kGy.

PU materials (Le Gac et al., 2013) was aged during 18 months in natural sea water and at different temperatures: 70, 90, 100, 110 and 120 °C. In regards to SR materials (Kashi et al., 2018), accelerated aging was performed by exposing samples to a functional oil (polyalkylene glycol) at an elevated temperature of 195 °C.

Time/temperature equivalence

Accelerated aging tests performed at temperatures well above real operating conditions allows significantly decreasing experimental time. Therefore, it is necessary to assume that the polymer properties resulting from high temperature and short time exposure, is analogous to that obtained after material being exposed to lower temperature but for longer times. This is the basis of the time–temperature equivalence principle which allows studying the evolution of mechanical, physical or chemical quantities in a reasonable time and extrapolating the results to much longer times.

The method consists in constructing a master curve on the basis of the tests carried out at different but high temperatures. The extrapolation from high temperatures (accelerated aging conditions) to lower temperatures (longer times) is achieved by using a shift factor a_T calculated from a reference temperature T_0.

Even if this equivalence remains questionable (Celina et al., 2005), it was successfully used in the literature (Gillen et al., 2006; Ha-Anh and Vu-Khanh, 2005; Rivaton et al., 2005a; Woo and Park, 2011) and two relationships for the shift factor are available.

In this work we have used that given by eq. (11) which takes the form of an Arrhenius power law.

$$ln(a_T) = -\frac{E_a}{R}\left(\frac{1}{T}-\frac{1}{T_0}\right) \tag{11}$$

In eq. (11), T is the absolute temperature, R the gas constant (8.314 J.K^{-1}.mol^{-1}) and E_a the activation energy expressed in kJ.mol^{-1}. We can note that this expression exhibits a physical meaning since the only parameter to identify is the energy activation which can be independently measured.

4.3. Swelling technique

The swelling method allows a direct measurement of the network degradation during aging. It consists in evaluating the capability of the network to absorb a liquid (solvent).

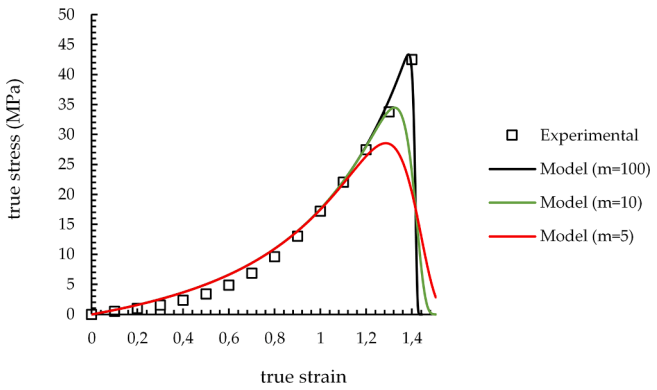

Fig. 1. Uniaxial tensile tension test of EPDM-01: comparison between the energy limiter approach and experimental data.

Table 1
Studied materials.

Materials	EPDM-01	EPDM-02	EPDM-03	PU	SR
Reference	This work	(De Almeida, 2014)		(Le Gac et al., 2013)	(Kashi et al., 2018)
Crosslinking agent	3phr, peroxide	3phr, peroxide	3phr, peroxide	–	–
Network structure	Amorphous	Amorphous	Semi crystalline	–	–
Filler	ATH	150phr of ATH	150phr of ATH	–	–
Degradation mechanism	crosslinking		chain scission		

Table 2
Available and deduced data.

Materials	Digitized data				Deduced data
EPDM-01 (De Almeida, 2014)	$Q(D)$	$\sigma(\varepsilon)$	$\varepsilon_b(D)$	$\sigma_b(D)$	ν
EPDM-02 (De Almeida, 2014)					
PU (Le Gac et al., 2013)	$\sigma(\varepsilon)$	$\varepsilon_b(t)$	$\sigma_b(t)$	$\nu(t)$	–
SR (Kashi et al., 2018)	$\sigma(\varepsilon)$	–	–	–	ν, $\sigma_b(t)$ and $\varepsilon_b(t)$
D: Dose absorbed	Q: swelling ratio	ν: EAC concentration	ε_b: stain at break		σ_b: stress at break

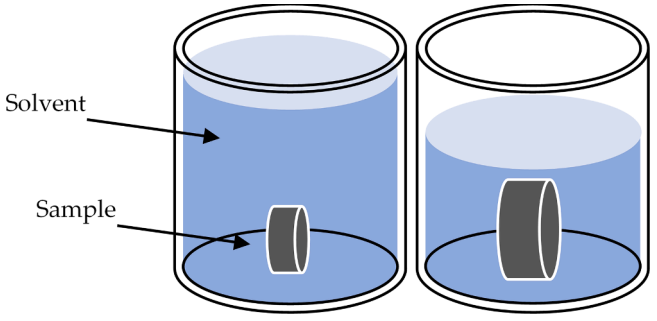

Fig. 2. Swelling test.

The tests were performed by swelling samples of approximately 40 mg weight until equilibrium in cyclohexane for 72 h when considering EPDM-01. While, for EPDM-02 and EPDM-03 materials, specimens were immersed during 192 h in xylene solvent (De Almeida, 2014).

For each aging state, the weights before and after swelling are measured. The polymer swelling ratio Q is deduced from the following relationship:

$$Q = 1 + \frac{\rho_{polymer}}{\rho_{solvent}} \frac{m_s - m_d}{m_d(1-\eta)} \quad (12)$$

where η is the mass fraction of fillers, m_d and m_s are respectively the mass of the dried specimen and that of the swollen specimen.

4.4. Mechanical tests

The mechanical properties of EPDM-01 such as tensile strength and elongation at break have been measured according to ISO 37: 2011 standard.

The tests were carried out on H3 type specimens, at ambient temperature 22 °C and under a constant cross-head speed of 50 mm/min. For each aging state, seven tests were carried out to check the scattering of the experimental data. The strain measurements were achieved by using an extensometer system.

Concerning EPDM-02 and EPDM-03 materials (De Almeida, 2014), the specimen geometry was a H2 type and the tensile tests were achieved by the respective authors at 2 different temperatures (25 and 80 °C) under a cross-head velocity of 12 mm/min. Between 3 and 5 tests per aging state were carried out, but only average values were reported (De Almeida, 2014).

The tensile tests of PU material (Le Gac et al., 2013) were carried out on samples of 2 mm thick haltere normalized forms, following the ISO 37 type 2 standard, an Instron machine was used with a 500 N load cell and with cross-head speed of 500 mm/min. for each exposure time 3 samples were tested (Le Gac et al., 2013).

Mechanical properties of SR material (Kashi et al., 2018) were determined through tensile test achieved using a Lloyd LR 30 K machine, equipped with a 1 kN load cell and under a crosshead speed of 200 mm/min. Measurements was carried out at ambient temperature and three dumbbell-shaped specimens were tested for each batch (Kashi et al., 2018).

5. Network alteration due to aging

5.1. Aging mechanisms

The chemical mechanisms of radio-oxidation and thermo-oxidation of EPDM materials are well known (Bolland and Gee, 1946; Decker et al., 1973; Rincon-Rubio et al., 2001; Rivaton et al., 2005a, 2005b; Tobolsky et al., 1950). They remain broadly similar, and they are described as a three-step chain reaction mechanism: initiation, propagation and termination.

Initiation consists in the creation of free radicals P°, these radicals being extremely reactive in the presence of oxygen O_2. This interaction creates a chain reaction of chemical processes in the polymer (propagation). The last step, which is termination, consists in transforming the different radicals (P° and PO_2°) from the previous step into inactive products (gas release, crosslink or scission), which lead to modifications of the initial polymer network.

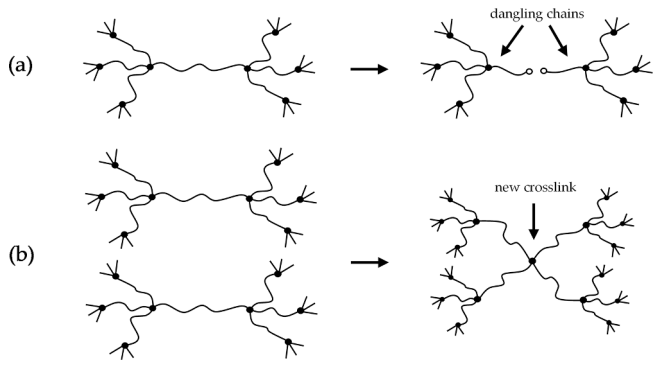

Fig. 3. (a) Chain scission and (b) crosslinking in the network: schematic.

The two main mechanisms which are involved are the scission and the crosslinking of the chains as schematically illustrated in Fig. 3. The predominance of each other in the degradation mechanisms is due to various factors, in particular to the chemical composition of the material (Belbachir et al., 2010; Hassine and Mouna, 2013; De Almeida, 2014; Planes, 2008; Shabani, 2013; Sidi, 2016).

5.2. Physical-chemical parameters representative of the network degradation

The molar mass between crosslinks M_c has often been used as a parameter of network damage during aging for materials that observe chain crosslinking. Indeed, the theory of the polymer chain directly relates the maximum extension of the chain to the average molar mass between crosslinks (Rami Bouaziz et al., 2020). However, when the chain scission operates in the network, the created dangling chains included in the measurement of M_c, do not contribute to the mechanical response of the elastomer network. Therefore, in this case, M_c is no longer a relevant parameter representative of the degradation when analysed through a mechanical point of view and other parameters must be involved.

5.2.1. Elastically active chains (EAC) concentration

When the crosslinking occurs in the network, the concentration of elastically active chains EAC noted ν increases and energy is thus better distributed. At the same time, the average length of the EACs decreases, thus limiting the maximum extensibility of the chains and consequently increases the hardening and the brittleness. The chain scission mechanism provokes a decrease of the EACs concentration and a simultaneous creation of dangling chains. Since the latter are not linked to the backbone, they do not contribute to the mechanical response. Thus, a softening of the material is the mechanical consequence of the chain scission.

Fig. 4a and Fig. 4b represent the evolution of the true stress and the true strain at break of EPDM-01 respectively, as a function of the reduced EAC concentration (ν_0 is the initial EAC concentration). Fig. 4c and Fig. 4d show the same data obtained for EPDM-02 and EPDM-03 material (De Almeida, 2014).

The predominant degradation mechanism is crosslinking in Fig. 4a and Fig. 4b, while chain scission dominates in Fig. 4c and Fig. 4d. Whatever the mechanism of degradation during aging, the stress at break decrease. When considering the strain at break, a decrease is observed for crosslinking mechanism while it is almost constant when chain scission prevails.

Different studies (Hassine and Mouna, 2013; De Almeida, 2014; Kartout, 2016; Planes, 2008; Pubellier, 2017; Shabani, 2013; Sidi, 2016) dealing with the effects of thermal and radiative aging on the mechanical properties at break of EPDMs confirms the above observations (Fig. 4).

The effects of the macromolecular network modifications on the properties at break have been studied by Mark (Andrady et al., 1981; Llorente and Mark, 1980; Mark, 2004). They proposed a network model made of different chain lengths. A drop of the elongation at break was noticed when the chain length becomes too short, which is similar to an increase of the network cross-linking. When the scissions occur, depending on the functionality of the network, the number of elastically active chains (EAC) decreases, and dangling chains are created. Consequently, the real network progressively and strongly deviates from the idealized one (Gillen et al., 1996), thus making the trends much more difficult to predict.

It can be assumed that chain scission mechanism generates subnetworks of different chain lengths, thus contributing to the

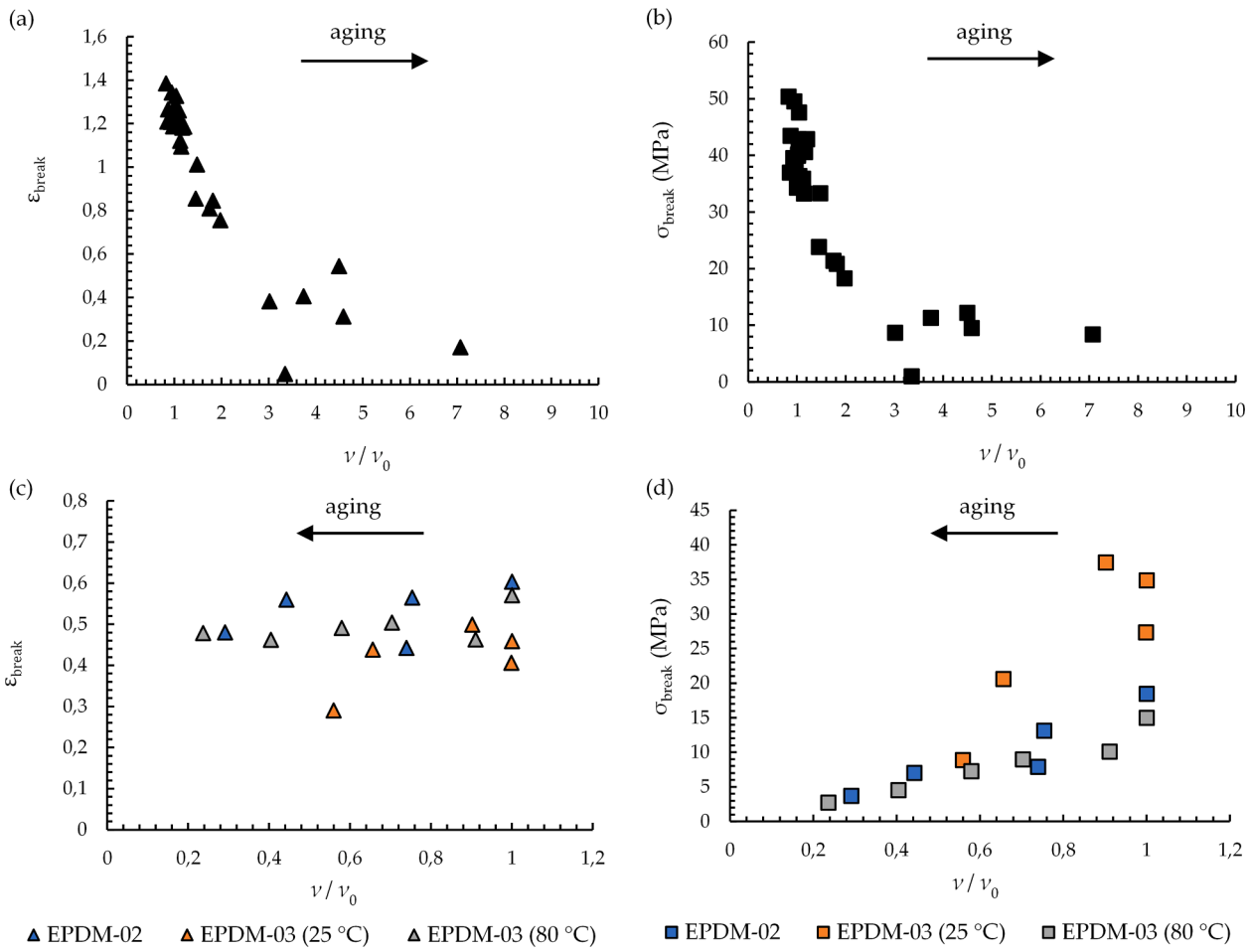

Fig. 4. Experimental evolution of EPDM failures properties: (a) and (b) crosslinking mechanism predominant, (c) and (d) chain scission mechanism predominant (De Almeida, 2014).

heterogeneity of the macromolecular network. When the network is loaded, the stress distribution is not uniform, the shortest chains being first to undergo the mechanical loading. When the stress level becomes too high, the shortest chains break which leads to an overloading of the other sub-networks. Consequently, a cascade break is generated.

5.2.2. EAC concentration measurements

The EAC concentration can be deduced from uniaxial tension tests by stiffness measurements:

$$\mu = \nu RT \tag{13}$$

The evolution of the shortest chains in the network has been analysed and reported in appendix. It concludes that the average concentration of elastically active chains in the network is a sufficient and relevant parameter to monitor the damage of the network.

5.2.3. Swelling rate Q as a damage parameter?

When analysing the swelling ratio evolution during aging, a decrease (crosslinking) or an increase (chain scission) of this parameter is observed. These results make this parameter a good candidate to be implemented as an alternative damage parameter in the mechanical modelling.

The measurement of the swelling ratio Q (eq. (12)), is a measurement which only requires a small size specimen and particularly useful for characterizing the degradation of elastomer networks (Hassine and Mouna, 2013; Kartout, 2016; Planes et al., 2010a; Planes et al., 2010b; Planes et al., 2009; Shabani, 2013). It could be preferred to tension tests when the sample is extracted from operating components.

The test consists in immersing an elastomer sample in a solvent (Fig. 2) for an enough required duration allowing reaching an equilibrium state.

The absorption of the solvent by the polymer creates an internal pressure, and due to the conformational abilities of the polymer, the chains of the network will tend to expand in the three-dimensional space. Equilibrium is reached when reaching the balance between internal pressure (due to the network deformation) and the hydrostatic pressure exerted by the solvent. This ability to swell is proportional to the free available volume in the elastomeric network during aging. Chain scission releases volume while cross-linking reduces free volume (Fig. 5).

5.3. Coupling the microstructural degradation to the mechanical model

When rubber material is manufactured following rubber vulcanization procedure, optimized properties at break are obtained. Therefore, a lack of crosslinking similar to chain scission or an excessive cross-linking will induce a decrease of properties at break (CORAN, 1994; Coran, 2003; Ghosh, 2003; Visakh and Thomas, 2013). Thus, we assume that the materials manufacturing has strictly followed the vulcanization procedure, and consequently the as received materials exhibits optimal properties at break. As discussed in Section 5.2.2 and Section 5.2.3, swelling ratio Q and EAC concentration ν can be considered as indicators of the degradation state of the network, which could be used as relevant parameter to characterize the network and its modifications during aging.

Accounting for the above considerations, the material failure energy

of rubber φ is assumed depending on one of cited damage parameter, and its evolution could be simply expressed as follows:

$$\varphi(\delta) = \varphi_0 \frac{\delta - \delta_t}{\delta_0 - \delta_t} \tag{14}$$

where δ is the chosen parameter (Q or ν), φ_0 and δ_t are respectively the material failure energy and the threshold value of the damage parameter, beyond which the material is supposed to be fully degraded. By fully degraded, we mean that the material could not undertake any load. Nevertheless, this threshold is a parameter that could be adjusted depending on the needing of the user especially if a more conservative estimate is required.

Because during aging, the two mechanisms can be involved, it seems us necessary to consider this phenomenon. Indeed, for example, when chain scission prevails, crosslinking can occur during the first stage of aging, often due to residues of the crosslinking agent which causes an additional crosslinking. That could be accounted for by expressing the failure energy in the following form:

$$\varphi(\delta) = H(\xi)\varphi_c(\delta) + H(\kappa)\varphi_s(\delta) \tag{15}$$

For example, if Q is the damage parameter, for two consecutive times t and $t+1$, ξ and κ take the following forms:

$$\begin{aligned} \xi &= Q_t - Q_{t+1} \\ \kappa &= Q_{t+1} - Q_t \end{aligned} \tag{16}$$

H is the Heaviside function:

$$H(z) = \begin{cases} 0 & , \quad z < 0 \\ 1 & , \quad z \geqslant 0 \end{cases} \tag{17}$$

φ_c and φ_s are the failure energy functions corresponding to cross-link and chain scission mechanisms, respectively.

6. Results and discussions

6.1. Degradation kinetics

Whatever the aging processes the evolution of the considered parameter (Q or ν) is fitted according to the following general equation:

$$\delta(X) = a\exp(b.X) + c\exp(d.X) \tag{18}$$

where δ is the considered parameter (swelling ratio Q or EAC concentration ν) and X is the variable (time t or absorbed dose D).

The parameters a, b, c and d are fitted using a square least method and the values for each material based on experimental data from Table 1 are reported in Table 3. Note that eq. (18) is not based on any physical consideration and can not be used as it is for other material/studies.

6.1.1. EPDM-01

Q values were determined through swelling tests as described in section 4.3. Its evolution as a function of exposure time at 150 °C is reported in Fig. 6a. Q monotonically decreases with aging time, thus highlighting chain crosslinking during thermo-oxidation.

The evolution of the concentration of EAC can be deduced from the uniaxial mechanical tests by using eq. (10). The obtained results are illustrated in Fig. 6b and show an exponential increase of this concentration with aging time (crosslinking mechanism).

6.1.2. EPDM-02

For this material, subjected to γ radiations, the swelling measurements as function of the absorbed dose, are reported in Fig. 7a. One can note that Q decreases between 0 kGy and approximately 210 kGy and then gradually increases until reaching high values for the maximum absorbed dose of 1000 kGy. The preliminary decrease observed for low doses is probably due to a crosslinking mechanism, which prevails because of the presence of peroxide residues in the matrix. Due to the competition between the two mechanisms, chain scission process gradually gains the upper hand and becomes predominant when increasing absorbed dose.

The measurements of EAC concentration are estimated through the shear modulus obtained from the mechanical tensile tests. The results are in agreement with the evolution of the swelling ratio Q described above. The major degradation mode, which is crosslinking observed at low doses of irradiation is evidenced by an increase in ν. Then, above approximately 210 kGy, chain scission mechanism becomes predominant, indicated by a decrease of node's concentration in the matrix.

6.1.3. EPDM-03

Similarly to EPDM-02, EPDM-03 materials (De Almeida, 2014) shows a slight decrease in the swelling ratio evolution between 0 and approximately 210 kGy, followed by an increase for higher doses, as highlighted in Fig. 8.

Since EPDM-03 (De Almeida, 2014) is a semi-crystalline material, the effects of the aging conditions on the solely matrix were separately captured by studying the unfilled material. The effects of the fillers were then analysed for the same aging conditions than that assigned to the pure matrix. The degradation kinetics of the unfilled matrix which shows the same trends than the EPDM-03 composite (De Almeida, 2014), confirms the above reported evolution, that is to say a slight decrease between 0 kGy and 210 kGy, then a gradual increase depending on the irradiation dose absorbed.

In the same way, the concentration of elastically active chains is deduced from the tensile tests at room temperature and at 80 °C. The obtained evolution is illustrated in Fig. 9.

6.1.4. PU and SR materials

The evolution of the network degradation for PU and SR materials is different compared to the previous materials. Indeed, we notice a monotonic decrease in EAC concentration throughout the aging period for both materials which is the marker of a prevalent chain scission mechanism (Fig. 10).

6.2. Predictive capability of the energy limiter model

Using the experimental data of the selected set of materials above described, the predictive capabilities of the energy limiter approach to capture the whole mechanical behaviour including the properties at break is discussed in this section.

The different parameters used in the model are summarized in Table 4.

Note that in Table 4, the subscript t_c and t_s means the threshold value of the parameter, for crosslinking and chain scission respectively.

6.2.1. EPDM-01

Fig. 11 shows the tensile curves of EPDM-01 for different exposure times at a temperature of 150 °C.

To describe the whole behaviour beyond the fracture, the evolution of the material failure energy during aging is required and is calculated using eq. (14). The parameters involved in this equation are: $Q_0 = 5.559$, $\varphi_0 = 18.45$ MPa which correspond to the swelling ratio and to the material failure energy of the as-received material, $Q_t = 2.8$ is the threshold swelling ratio, corresponding to the fully degraded material. Fig. 11

shows a quite good agreement between the experimental data and the evolution predicted by the model. Even only the data for one aging temperature are shown, the same trends are observed for the other aging temperatures.

A nice agreement can be observed between the experimental results and the estimates given by the energy limiter approach in Fig. 11 and Fig. 12, thus demonstrating the relevance of the model in the prediction of properties at break of a material which crosslinks during aging.

In Fig. 12, the time–temperature equivalence, based upon the Arrhenius power law given by eq. (11), was applied to build the master curve during aging. The activation energy value giving the best fit of the data was found equal to $E_a = 95$ kJ/mol.

Stress at break, corresponding to the maximum value reached by the stress evolution, is deduced from eq. (10) for each aging state. The model estimates calculated by using the swelling ratio parameter as the damage parameter (referred as model (Q) in Fig. 12) are compared to the experimental data in Fig. 12a. Even the experimental data are quite scattered, the trend is well captured by the model, confirming the relevance of the energy limiter approach.

This relevance is also depicted in Fig. 12b, when analysing the evolution of the strain at break which can be evaluated again from eq. (10) by using a Newton method.

Note that when the average concentration of EAC is taken as the damage parameter (referred as model (ν) in Fig. 12), a satisfactory agreement is also depicted.

6.2.2. EPDM-02

Since the two modes of degradation are observed (scission and crosslinking) for EPDM-02 material (De Almeida, 2014), eq. (15) is more suitable to predict failure properties evolution.

A comparison between experimental data and model estimates is shown in Fig. 13, in terms of stress versus strain curves. The obtained results confirm the capability of this approach to account for the two degradation mechanisms in the description of the mechanical behaviour including the fracture process Fig. 14.

For this material, the evolution of the stresses at break during aging is more sensitive than that of the corresponding strains. Indeed, we can notice that the stresses decrease continuously with respect to aging while the deformations exhibit a decrease in the first stage of aging due to an additional crosslinking of the network, then remains quite constant. The model well captures these evolutions but predict a sudden drop in the strain evolution indicating a full degradation of the material. Thus, this analysis shows that a stress-based criterion is preferable when designing the rubber components, when chain scission is the prevalent degradation mechanism.

6.2.3. EPDM-03

Because this material is semi-crystalline, it was studied at two temperatures: at 80 °C (Fig. 15a) for which it exhibits an amorphous structure and at 25 °C (Fig. 15b) for which the structure is semi-crystalline.

Note that at 80 °C, that is to say when the material is completely amorphous, the stiffness of the material decreases continuously with the level of absorbed dose. This suggests that the drop in swelling ratio at low doses seen in Fig. 8 is not only due to matrix crosslinking but also to crystallization. Indeed, De Almeida (De Almeida, 2014), by investigating the crystallinity evolution χ_c of EPDM-03 material (De Almeida, 2014) during aging, has observed an increase of χ_c ($+4.4 \pm 1\%$) between 0 kGy and 450 kGy, followed by a decrease at higher doses, confirming that the structural changes in the elastomer network were not only due to crosslinking.

The results obtained for EPDM-03 (De Almeida, 2014) at 80 °C and 25 °C, using the same values of thresholds parameters in the failure energy function based on swelling ratio variations, whatever the material structure (amorphous or semi-crystalline), show a good agreement between model prediction and experimental data. Thus, the results obtained Fig. 15 (a) and (b) show that the properties at break are monitored rather by the amorphous phase, than the crystalline phase, provided the degree of crystallinity remains relatively low.

A comparison between the experimental data at 80 and 25 °C, and the model estimates in terms of stress and strain at break are respectively shown in Fig. 16 and Fig. 17. Again, a very nice agreement is highlighted, demonstrating the relevance of the approach and confirming the capability of the model to take into account the degradation mechanisms (crosslinking and chain scission).

Thus, the model offers the possibility of estimating the lifetime of EPDM components, when the end-of-life criterion of these components is based on the properties at break.

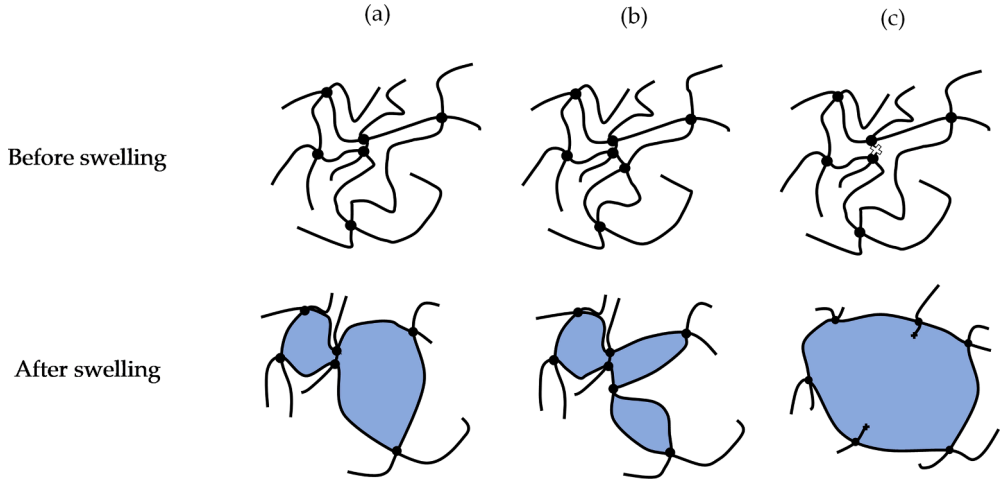

Fig. 5. Effect of a random (b) crosslink and a random chain scission (c) on network swelling compared to the initial state (a) (schematic).

Table 3
Fitting parameter values.

Materials	Considered parameter	a	b	c	d
EPDM-01	Q (–)	6.69	0	$-9.05.\ 10^{-1}$	$6.95.\ 10^{-2}$
	ν (mol/cm^3)	10^{-3}	0	$8.0.\ 10^{-5}$	$1.5.\ 10^{-1}$
EPDM-02 (De Almeida, 2014)	Q (–)	0.88	$-2.9.\ 10^{-3}$	1.57	$7.77.\ 10^{-4}$
	ν (mol/cm^3)	$6.75.\ 10^{-3}$	$-2.2.\ 10^{-3}$	$-4.81.\ 10^{-3}$	$-4.89.\ 10^{-3}$
EPDM-03 (De Almeida, 2014)	Q (–)	1.165	$-1.37.\ 10^{-3}$	1.12	$9.44.\ 10^{-4}$
	ν (mol/cm^3) (25 °C)	$1.39.\ 10^{-2}$	$-1.35.\ 10^{-3}$	$-7.5.\ 10^{-3}$	$-4.4.\ 10^{-3}$
	ν (mol/cm^3) (80 °C)	$4.94.\ 10^{-3}$	0	$-2.85.\ 10^{-3}$	$4.5.\ 10^{-4}$
PU (Le Gac et al., 2013)	ν (mol/cm^3)	$3.04.\ 10^{-3}$	$-4.5.\ 10^{-2}$	0	0
SR (Kashi et al., 2018)	ν (mol/cm^3)	$8.49.\ 10^{-5}$	$-5.89.\ 10^{-2}$	0	0

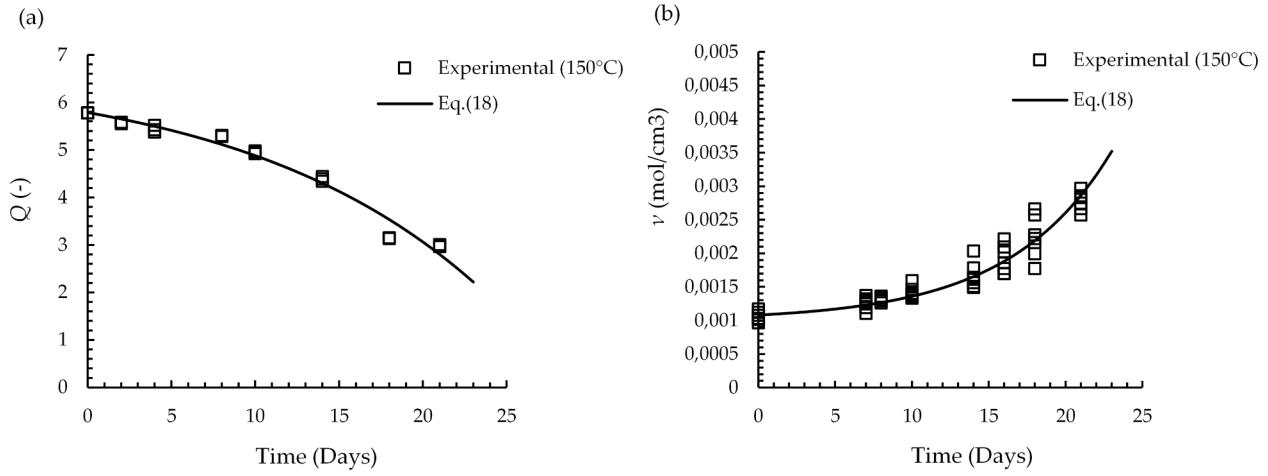

Fig. 6. Evolution of the swelling ratio (a) and of the EAC concentration ν as a function of exposure time at 150 °C.

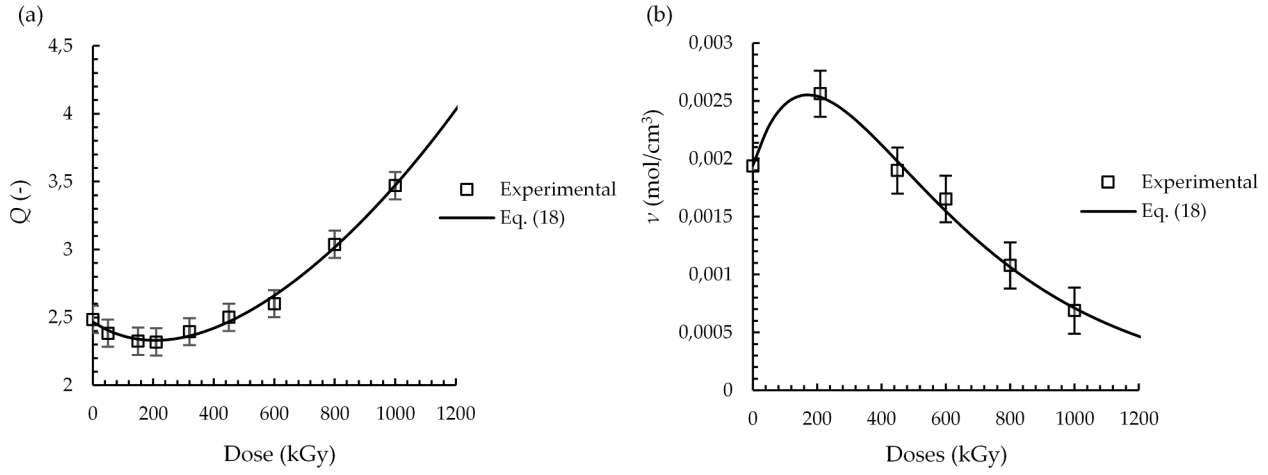

Fig. 7. Evolution of the swelling ratio Q and of the EAC concentration ν as a function of the absorbed dose for EPDM-02 (Experimental: (De Almeida, 2014), modelling: this work).

Table 4
Parameter value of the model.

Materials	Eq. (10)		Eq. (14) or Eq. (15)	
	N_0	φ_0 (MPa)	Q_t (–)	ν_t (mol/cm^3)
EPDM-01	21	18.45	2.8	$2.8.\ 10^{-3}$
EPDM-02 (De Almeida, 2014)	25	6.8	$Q_{tc} = 1.9$, $Q_{ts} = 3.8$	$\nu_{tc} = 4.5.\ 10^{-3}$, $\nu_{ts} = 4.\ 10^{-4}$
EPDM-03 (80 °C) (De Almeida, 2014)	18.5	4.15	$Q_{tc} = 2.17$, $Q_{ts} = 3.5$	$\nu_t = 2.\ 10^{-4}$
EPDM-03 (25 °C) (De Almeida, 2014)	10	13.2		$\nu_{tc} = 9.\ 10^{-3}$, $\nu_{ts} = 2.6.\ 10^{-3}$
PU (Le Gac et al., 2013)	120	42	–	$\nu_t = 4.36.\ 10^{-2}$
SR (Kashi et al., 2018)	345	62.5	–	$\nu_t = 5.81.\ 10^{-5}$

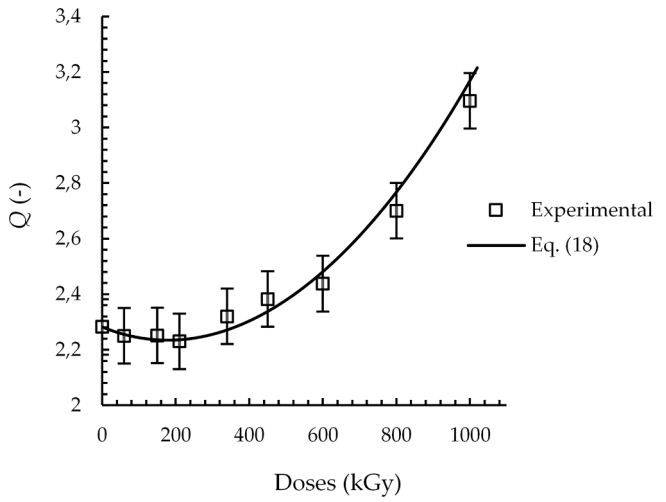

Fig. 8. Evolution of EPDM-03 swelling ratio Q during aging as function of the absorbed dose (Experimental: (De Almeida, 2014), modelling: this work).

6.2.4. *PU and SR*

The prediction of the properties at break of PU (Le Gac et al., 2013) and SR (Kashi et al., 2018) materials (Fig. 18 and Fig. 19) is done by using the EAC concentration as the damage indicator, because swelling data are not available. Again, the energy limiter approach leads to quite satisfactory predictions except for PU material (Le Gac et al., 2013) for which the early increase of the strain at break is not captured by the model. In this case, this one is subjected to hydrolysis aging which means that the initial state varies with the consumption of salt water.

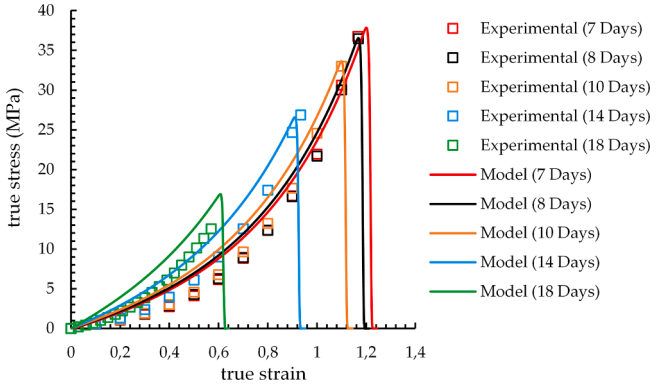

Fig. 11. True stress as function of true strain of EPDM-01 for different time exposures at 150 °C (dots: experimental, lines: eq. (10)).

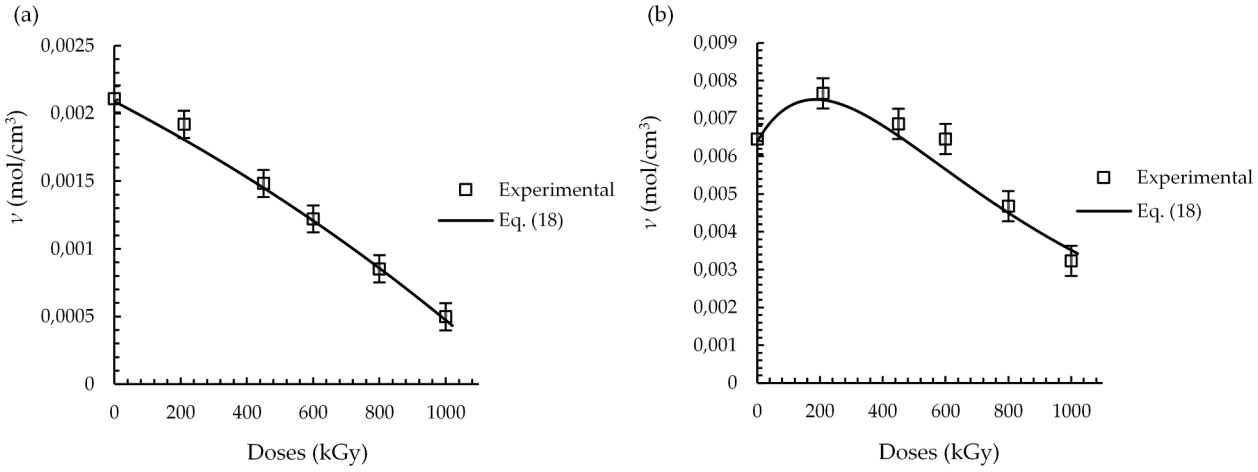

Fig. 9. Evolution of the elastically active chains concentration during radio-oxidative aging for EPDM-03 at (a) 80 °C and (b) 25 °C (Experimental: (De Almeida, 2014), modelling: this work).

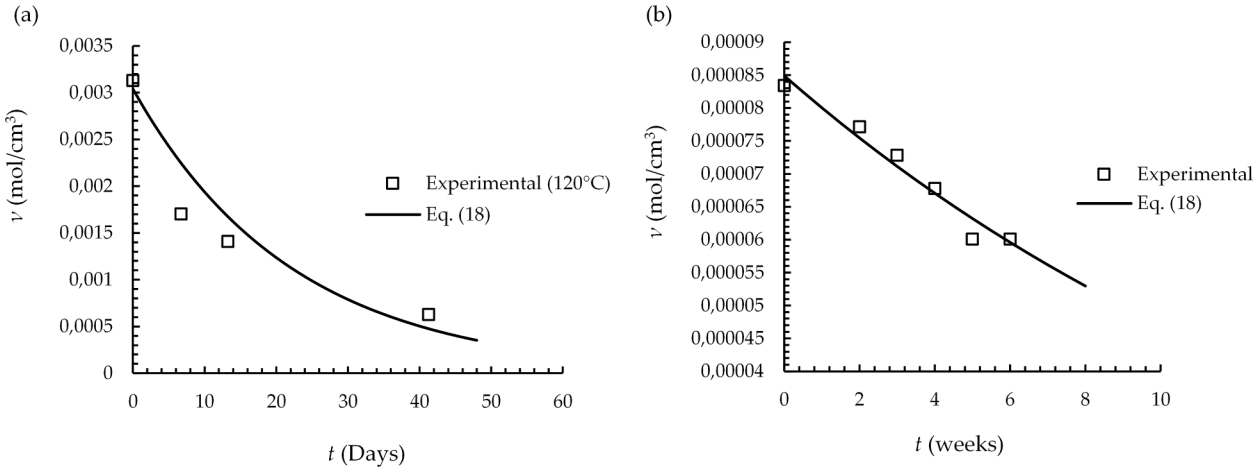

Fig. 10. Evolution of EAC concentration during aging for (a) PU and (b) SR materials (Experimental: (a) (Le Gac et al., 2013) (b) (Kashi et al., 2018), modelling: this work).

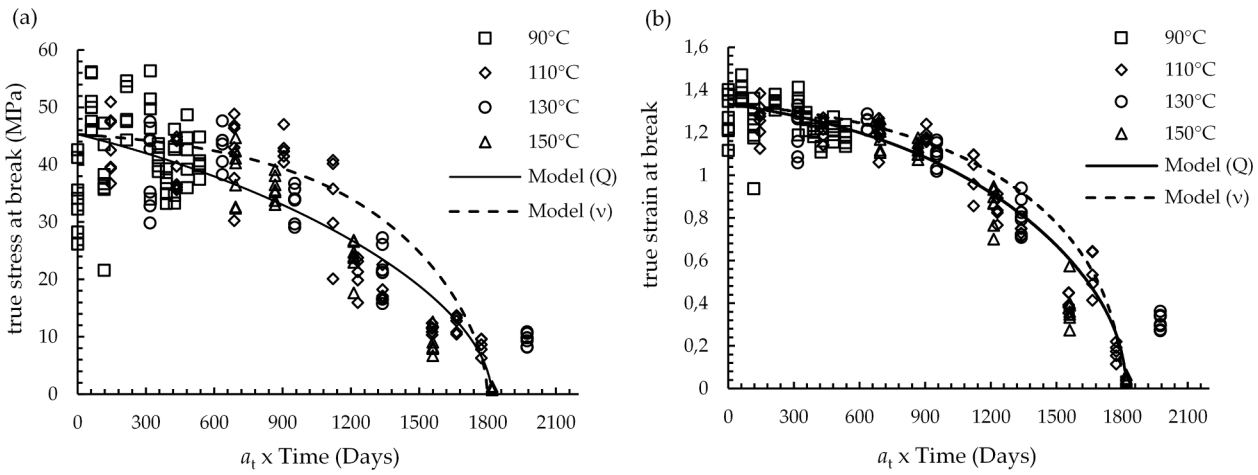

Fig. 12. True strain and true stress at break as a function of the reduced time ($t \times a_t$): comparison between experimental data and modelling.

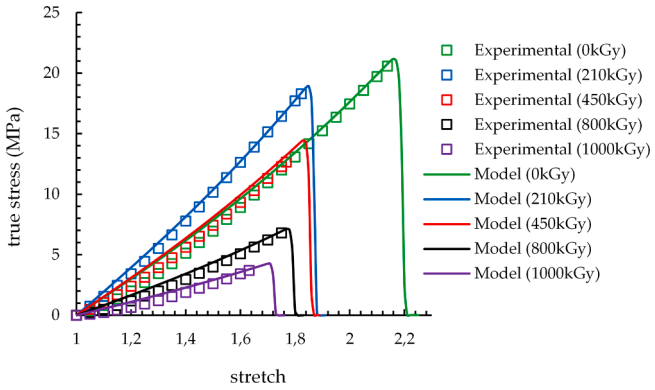

Fig. 13. True stress as function of true strain of EPDM-02 (De Almeida, 2014) for different absorbed doses (dots: experimental, lines: eq. (10)).

Indeed, the water absorption depends on both time and temperature which make the results more difficult to analyse. Nevertheless, the model is able in this case to well capture the evolution of the stress at break (Fig. 18a). Note that for PU material, the Arrhenius time–temperature equivalence was used ($E_a = 120$ kJ/mol).

7. Conclusion

In this work, the energy limiter approach was applied and extended for predicting the properties at break of rubber materials subjected physical–chemical aging. By analysing the data of different materials, some of them given in the literature, we have developed a general approach suitable whatever the aging mechanism involved in the material.

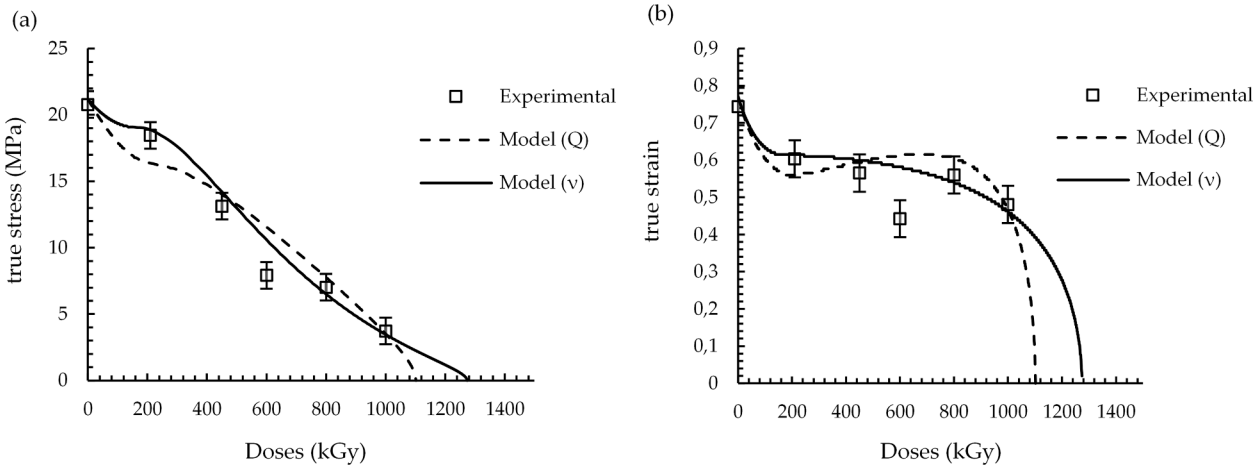

Fig. 14. True strain and true stress at break as function of the absorbed dose for EPDM-02 (De Almeida, 2014) : comparison between experimental data and modelling.

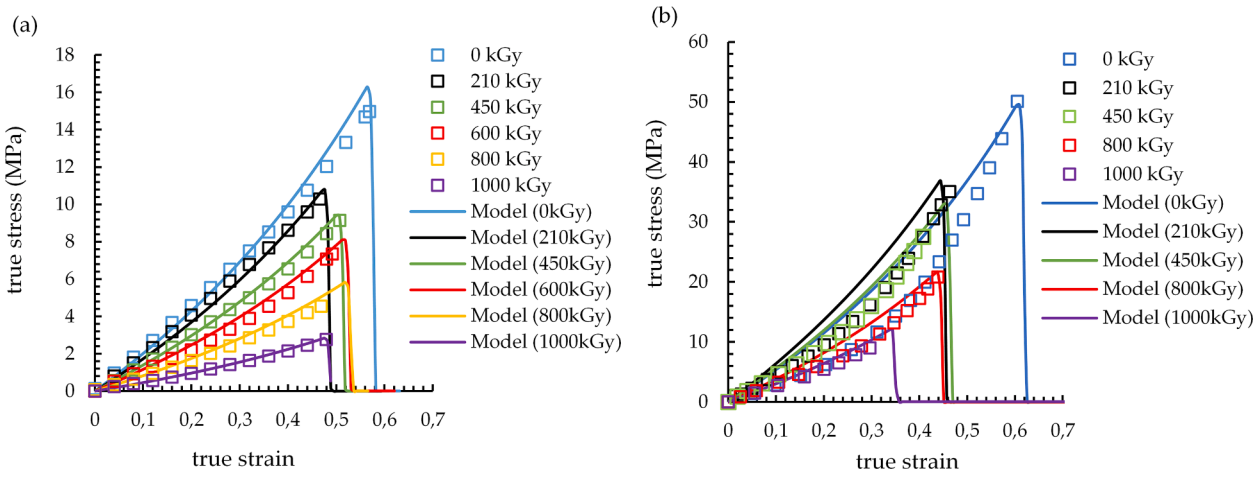

Fig. 15. True stress as function of true strain of EPDM-03 (De Almeida, 2014) for different absorbed doses at (a) 80 °C and (b) 25 °C (dots: experimental (De Almeida, 2014), lines: eq. (10)).

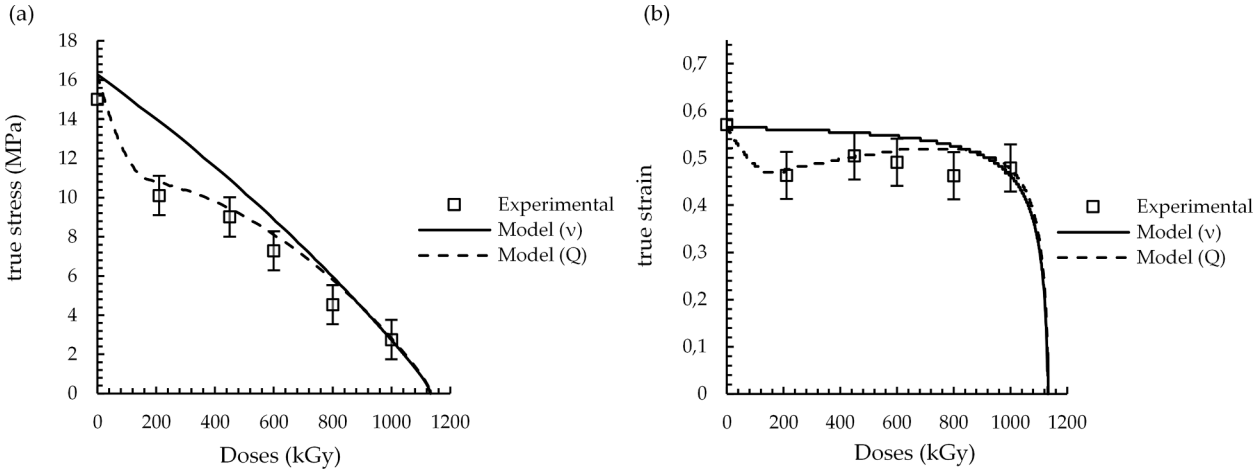

Fig. 16. True strain and true stress at break as function of the absorbed dose for amorphous EPDM-03 (De Almeida, 2014): comparison between experimental data (De Almeida, 2014) and modelling.

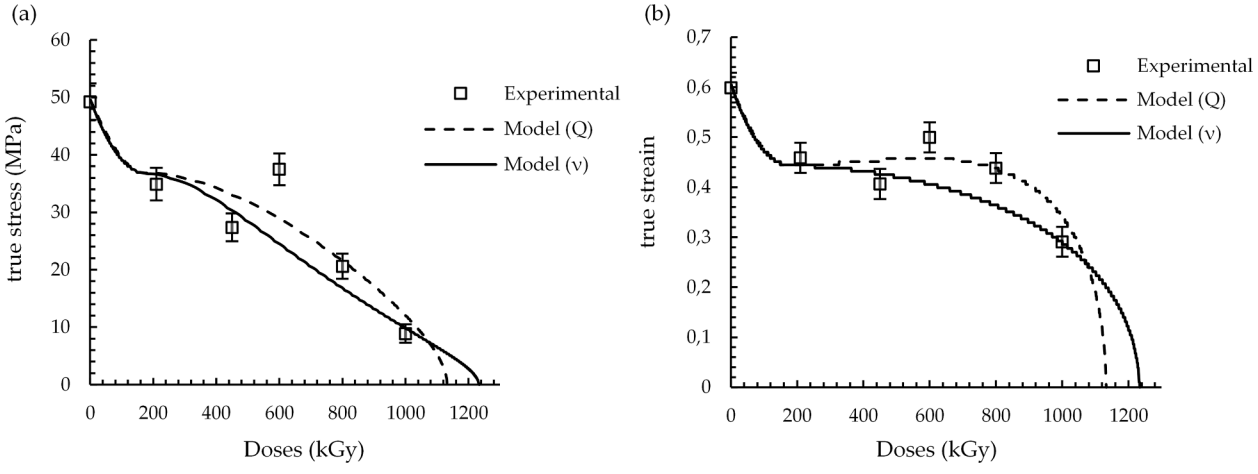

Fig. 17. True strain and true stress at break as function of the absorbed dose for semi-crystalline EPDM-03 (De Almeida, 2014): comparison between experimental data (De Almeida, 2014) and modelling.

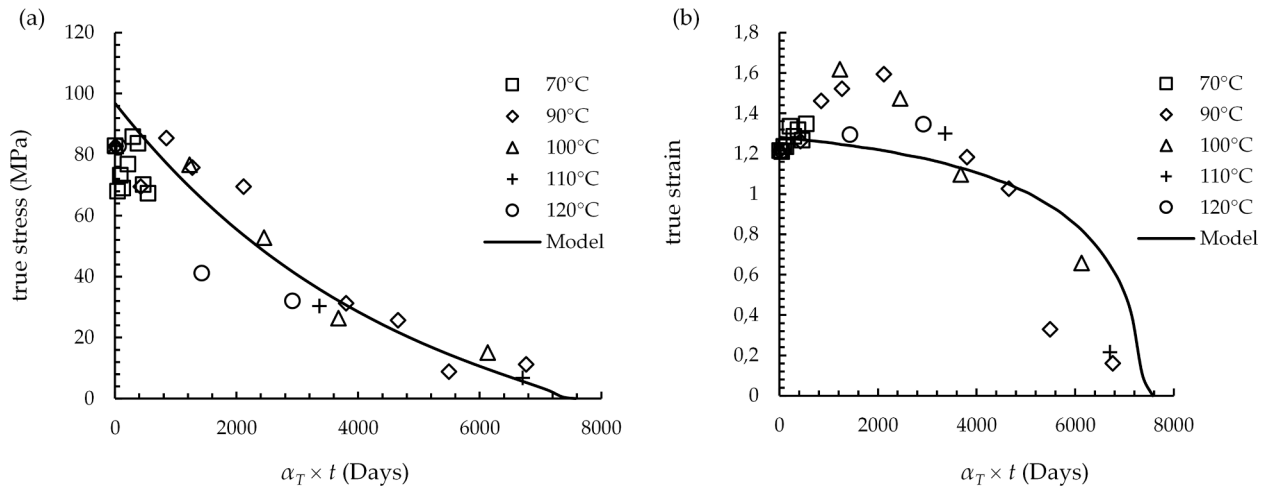

Fig. 18. True strain and true stress at break as function of exposure time for PU material (P.Y. Le Gac et al., 2013): comparison between experimental data (Le Gac et al., 2013) and modelling.

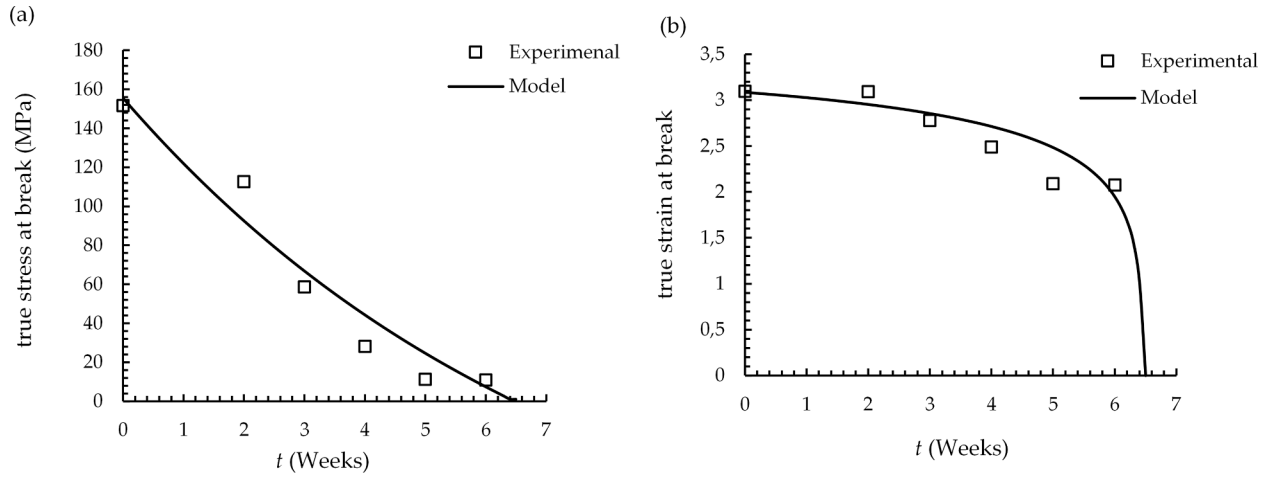

Fig. 19. True strain and true stress at break as function of exposure time for SR material (Kashi et al., 2018): comparison between experimental data (Kashi et al., 2018) and modelling.

Indeed, we have shown that EAC concentration is a relevant indicator of the degradation, whatever the aging mechanism, either cross-linking or chain scission. We have also shown that the swelling ratio, follows the inverse evolution than the EAC concentration during aging. It was established that it is also a relevant parameter able to capture the damage evolution.

Further, by extending the energy limiter approach, the capabilities of the model to capture the whole mechanical behaviour including the properties at break were investigated. Elastically active chain concentration and swelling ratio evolution were introduced in the model to fit the degradation process taking place during aging. The first parameter controls both the elastic behaviour of the material and the ultimate properties, while the second is only concerned with the properties at break.

We have shown that the damage evolution (described alternatively by the EAC concentration or the swelling ratio) can be approximated in a first step by a linear function requiring two parameters to be identified (an initial value corresponding to the as-received material and a threshold value linked to a fully degraded material).

Whatever the studied material and whatever the degradation mechanism, when comparing experimental results and estimates given by the proposed approach, a nice agreement was depicted, either for the evolution of the mechanical response or for the properties at break.

It makes the energy limiter approach a very useful tool for designing rubber components especially when subjected to aging process.

Declaration of Competing Interest

The authors declare that they have no known competing financial interests or personal relationships that could have appeared to influence the work reported in this paper.

Acknowledgements

The authors would like to thank the french agency ANRT (Association Nationale Recherche Technologie) and Electricité de France for their financial support of this research.

Appendix A

The determination of the EAC concentration can be achieved either by using the initial stiffness of the material (via uniaxial tension tests) or by analysis of the swelling property of the material immersed in a solvent (physical chemical method). Since the objective is to predict fracture which is monitored by the short chains, we focus on the determination of the EAC concentration which functionality is greater than 3.

By analysing the results, it is shown that these complex calculations are not necessary to provide good estimates of the fracture properties.

The chain scission mechanism induces EAC evolution which can be written as follows:

$$\nu = \nu_0 - \alpha\, s \tag{9.1}$$

where s is the number of scissions, and α a parameter which depends on the functionality f of the nodes (by means the number of chains attached to the node):

$\alpha = 3 \rightarrow f = 3$
$\alpha = 1 \rightarrow f > 3$

The functionality cannot be directly measured and is often taken equal to 3.5 or 4 (Valentín et al., 2008).

Theoretically, the more the density of the network crosslinking is high, corresponding to high functionality value f, the shorter the chains. Langley (Langley, 1969; Langley, 1968; Langley and Polmanteer, 1974) proposed a statistical description of the nodes concentration in the network and developed a relationship to describe the evolution of the EAC density, written as follows:

$$\nu = \underbrace{(q\rho/M_0)(1-F_s)\left(1-\sqrt{F_s}\right)^2}_{\nu_c} + \underbrace{2 \in \left(1-\sqrt{F_s}\right)^4}_{\nu_{trapped}} \tag{9.2}$$

The parameters q, F_s, M_0 and ϵ are the probability that a monomer is chemically modified, the soluble fraction, the monomer unit mass and the effective entanglement concentration, respectively.

When considering the right-hand side of eq. (9.2) ν_c corresponds to the contribution of chemical nodes and is equal to $\nu_{swelling}$, while $\nu_{trapped}$ is the concentration of physical nodes (entanglements).

$\nu_{swelling}$ is assessed through the following relationship (Kraus, 1963):

$$\nu_{swelling} = \frac{V_{r_0}}{V_s}\frac{V_r + \chi V_r^2 + ln(1-V_r)}{\left(\frac{2V_r}{f} - V_r^{1/3}V_{r_0}^{2/3}\right)} \tag{9.3}$$

where χ, V_s, V_r and V_{r0} are Huggins solvent-polymer interaction parameter, molar volume of solvent, apparent volume fraction of polymer in swelled composite and volume fraction of polymer in swelled gel, respectively.

The effective entanglement concentration ϵ can be determined empirically by plotting the evolution of EAC concentration ν_{mech} as a function of $\nu_{swelling}$, which can be determined through mechanical and swelling measurements respectively. According to eq. (9.4), the obtained evolution can be fitted by a straight line, which intercept with the y-axis corresponds to ϵ and which slope is the g value.

$$\frac{E}{3} = \nu_{mech}RT = g\nu_{swelling}RT \tag{9.4}$$

E is the initial elastic modulus corresponding to infinitesimal strain, R is the gas constant and T the absolute temperature.

According to Langley, mainly two kinds of crosslinking are present in the network, which nodes are tetra functional (f *greater than 3*) or tri-functional ($f = 3$). Their respective concentrations ν_{tetra} and ν_{tri} are related by the following expression:

$$\nu_c = \nu_{tri} + 2\nu_{tetra} \tag{9.5}$$

And

$$\nu_{tetra} = \left(\frac{q\rho}{2M_0}\right)\left(1-\sqrt{F_s}\right)^4 \tag{9.6}$$

$$\nu_{tri} = \left(\frac{q\rho}{M_0}\right)(1-F_s)\left(1-\sqrt{F_s}\right)^2 - \left(1-\sqrt{F_s}\right)^4 \tag{9.7}$$

Reminding that tetra-functional sub-network is assumed driving the behaviour at failure, above equations allows following the evolutions in the concentration of both tetra-functional and tri-functional nodes, which makes possible to assign the value of parameter α of eq. (9.1), and therefore to estimate the evolution of the number of scissions in the network.

The theory described by Langley and Polmanteer (1974) was applied to the matrix of the EPDM-02 material (Almeida, 2014), which was subjected to radioactive aging. The different concentrations were calculated and their evolution as a function of the absorbed dose is shown in Fig. 20.

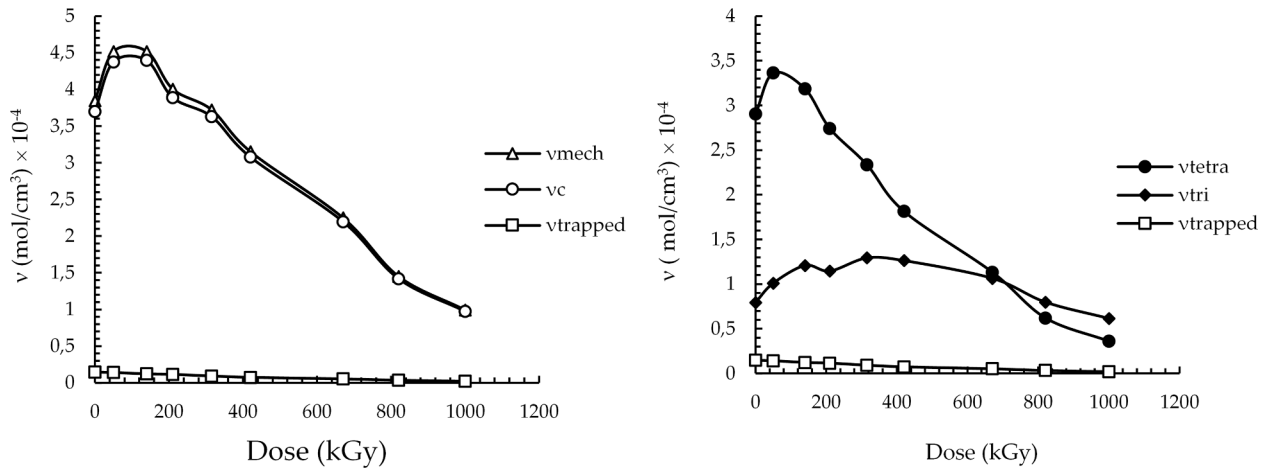

Fig. 20. Distribution of the elastically active chains concentration in the matrix for EPDM-02 (De Almeida, 2014).

The results show that the evolution of tetra-functional nodes concentration ν_{tetra} follows the same trends as ν_{mech} and ν_c. Thus, ν_{mech} seems to be a sufficient relevant parameter to describe the degradation of the network, and therefore allows avoiding additional calculations.

References

Andrady, A.L., Llorente, M.A., Sharaf, M.A., Rahalkar, R.R., Mark, J.E., Sullivan, J.L., Yu, C.U., Falender, J.R., 1981. Model networks of end-linked polydimethylsiloxane chains. XII. Dependence of ultimate properties on dangling-chain irregularities. J. Appl. Polym. Sci. 26 (6), 1829–1836.

Arruda, E.M., Boyce, M.C., 1993. A three-dimensional constitutive model for the large stretch behavior of rubber elastic materials. J. Mech. Phys. Solids 41 (2), 389–412.

Ayoub, G., Naït-Abdelaziz, M., Zaïri, F., Gloaguen, J.M., Charrier, P., 2011. A continuum damage model for the high-cycle fatigue life prediction of styrene-butadiene rubber under multiaxial loading. Int. J. Solids Struct. 48 (18), 2458–2466.

Ayoub, G., Naït-Abdelaziz, M., Zaïri, F., 2014. Multiaxial fatigue life predictors for rubbers: application of recent developments to a carbon-filled SBR. Int. J. Fatigue 66, 168–176.

Belbachir, S., Zaïri, F., Ayoub, G., Maschke, U., Naït-Abdelaziz, M., Gloaguen, J.M., Benguediab, M., Lefebvre, J.M., 2010. Modelling of photodegradation effect on elastic-viscoplastic behaviour of amorphous polylactic acid films. J. Mech. Phys. Solids 58 (2), 241–255.

Ben Hassine, M., Naït-Abdelaziz, M., Zaïri, F., Colin, X., Tourcher, C., Marque, G., 2014. Time to failure prediction in rubber components subjected to thermal ageing: a combined approach based upon the intrinsic defect concept and the fracture mechanics. Mech. Mater. 79, 15–24.

Ben Hassine, Mouna. 2013. 'Modélisation Du Vieillissement Thermique et Mécanique d'une Protection Externe En EPDM de Jonctions Rétractables à Froid'. Mécanique-Matériaux. École Nationale Supérieure d'Arts et Métiers. https://pastel.archives-ouvertes.fr/pastel-00941411.

Bolland, J.L., Gee, G., 1946. Kinetic studies in the chemistry of rubber and related materials. II. The kinetics of oxidation of unconjugated olefins. Trans. Faraday Soc. 42, 236. https://doi.org/10.1039/tf9464200236.

Bouaziz, R., Ahose, K.D., Lejeunes, S., Eyheramendy, D., Sosson, F., 2019. Characterization and modeling of filled rubber submitted to thermal aging. Int. J. Solids Struct. 169, 122–140.

Bouaziz, R., Truffault, L., Borisov, R., Ovalle, C., Laiarinandrasana, L., Miquelard-Garnier, G., Fayolle, B., 2020. Elastic properties of polychloroprene rubbers in tension and compression during ageing. Polymers 12 (10), 2354. https://doi.org/10.3390/polym12102354.

Celina, M., Gillen, K.T., Assink, R.A., 2005. Accelerated aging and lifetime prediction: review of non-arrhenius behaviour due to two competing processes. Polym. Degrad. Stab. 90 (3), 395–404.

Cohen, A., 1991. A padé approximant to the inverse langevin function. Rheol. Acta 30 (3), 270–273.

Colin, X., Hassine, M.B., Nait-Abelaziz, M., 2019. Chemo-mechanical model for predicting the lifetime of EPDM rubbers. Rubber Chem. Technol. 92 (4), 722–748.

Coran, A.Y., 2003. Chemistry of the vulcanization and protection of elastomers: a review of the achievements. J. Appl. Polym. Sci. 87 (1), 24–30.

Coran, A.Y., 1994. In: Science and technology of rubber. Elsevier, pp. 339–385 https://linkinghub.elsevier.com/retrieve/pii/B9780080516677500123 (July 21, 2020).

Dal, H., Kaliske, M., 2009. A micro-continuum-mechanical material model for failure of rubber-like materials: application to ageing-induced fracturing. J. Mech. Phys. Solids 57 (8), 1340–1356.

De Almeida. 2014. Propriétés Mécaniques et Dégradation Des Élastomères EPDM Chargés ATH. Matériaux. Institut National des Sciences Appliquées de Lyon. http://theses.insa-lyon.fr/publication/2014ISAL0053/these.pdf.

Decker, C., Mayo, F.R., Richardson, H., 1973. Aging and degradation of polyolefins. III. Polyethylene and ethylene-propylene copolymers. J. Polymer Sci.: Polymer Chem. Ed. 11 (11), 2879–2898.

Ehrenstein, G.W., Pongratz, S. (Eds.), 2007. Beständigkeit von Kunststoffen. Carl Hanser Verlag GmbH & Co. KG, München.

Gabrielle, B., Lorthioir, C., Lauprêtre, F., 2011. Thermal aging of interfacial polymer chains in ethylene–propylene–diene terpolymer/aluminum hydroxide composites: Solid-state NMR study. J. Phys. Chem. B 115 (43), 12392–12400.

Ghosh, Prasenjeet et al., 2003. Sulfur vulcanization of natural rubber for benzothiazole accelerated formulations: from reaction mechanisms to a rational kinetic model. *Rubber Chem. Technol.* 76(3): 592–693.

Gillen, K.T., Clough, R.L., Wise, J., 1996. Prediction of elastomer lifetimes from accelerated thermal-aging experiments. In: Clough, R.L., Billingham, N.C., Gillen, K. T. (Eds.), Polymer durability, Advances in Chemistry. American Chemical Society, Washington, DC, pp. 557–575.

Gillen, K.T., Bernstein, R., Clough, R.L., Celina, M., 2006. Lifetime predictions for semi-crystalline cable insulation materials: I. Mechanical properties and oxygen consumption measurements on EPR materials. Polym. Degrad. Stab. 91 (9), 2146–2156.

Ha-Anh, T., Vu-Khanh, T., 2005. Prediction of mechanical properties of polychloroprene during thermo-oxidative aging. Polym. Test. 24 (6), 775–780.

Hamdi, A., Naït Abdelaziz, M., Aït Hocine, N., Heuillet, P., Benseddiq, N., 2006. A fracture criterion of rubber-like materials under plane stress conditions. Polym. Test. 25 (8), 994–1005.

Hamdi, A., Naït Abdelaziz, M., Aït Hocine, N., Heuillet, P., Benseddiq, N., 2007. A new generalized fracture criterion of elastomers under quasi-static plane stress loadings. Polym. Test. 26 (7), 896–902.

Heinrich, G., E. Straube, G. Helmis. 1988. Rubber elasticity of polymer networks: theories. In *Polymer Physics*, Berlin, Heidelberg: Springer Berlin Heidelberg, 33–87. http://www.springerlink.com/index/10.1007/BFb0024050 (March 12, 2019).

Kartout, C., 2016. Vieillissement thermo-oxydant et rupture d'un EPDM. Université Pierre et Marie Curie, Physique-chimie des matériaux https://tel.archives-ouvertes.fr/tel-01359258.

Kashi, S., Varley, R., De Souza, M., Al-Assafi, S., Di Pietro, A., de Lavigne, C., Fox, B., 2018. Mechanical, thermal, and morphological behavior of silicone rubber during accelerated aging. Polymer-Plastics Technol. Eng. 57 (16), 1687–1696.

Kraus, G., 1963. Swelling of filler-reinforced vulcanizates. J. Appl. Polym. Sci. 7 (3), 861–871.

Lake, G.J., 2003. Fracture mechanics and its application to failure in rubber articles. Rubber Chem. Technol. 76 (3), 567–591.

Langley, N.R., 1969. Elastically effective strand density in polymer networks. Rubber Chem. Technol. 42 (5), 1285–1293.

Langley, N.R., 1968. Elastically effective strand density in polymer networks. Macromolecules 1 (4), 348–352.

Langley, N.R., Polmanteer, K.E., 1974. Relation of elastic modulus to crosslink and entanglement concentrations in rubber networks. J. Polymer Sci.: Polymer Phys. Ed. 12 (6), 1023–1034.

Le Gac, P.Y., Broudin, M., Roux, G., Verdu, J., Davies, P., Fayolle, B., 2014. Role of strain induced crystallization and oxidative crosslinking in fracture properties of rubbers. Polymer 55 (10), 2535–2542.

Le Gac, P.Y., Choqueuse, D., Melot, D., 2013. Description and modeling of polyurethane hydrolysis used as thermal insulation in oil offshore conditions. Polym. Test. 32 (8), 1588–1593.

Llorente, M.A., Mark, J.E., 1980. Model networks of end-linked poly (dimethylsiloxane) chains. 8. Networks having cross-links of very high functionality. Macromolecules 13 (3), 681–685.
Marckmann, G., Verron, E., 2006. Comparison of hyperelastic models for rubber-like materials. Rubber Chem. Technol. 79 (5), 835–858.
Mark, James et al. 2004. *Physical Properties of Polymers*. http://adsabs.harvard.edu/abs/2004ppp.book....M (April 27, 2019).
Miehe, C., 2004. A micro-macro approach to rubber-like materials? Part I: The non-affine micro-sphere model of rubber elasticity. J. Mech. Phys. Solids 52 (11), 2617–2660.
Miehe, C., Göktepe, S., 2005. A micro-macro approach to rubber-like materials. Part II: the micro-sphere model of finite rubber viscoelasticity. J. Mech. Phys. Solids 53 (10), 2231–2258.
Nait Abdelaziz, M., Ayoub, G., Colin, X., Benhassine, M., Mouwakeh, M., 2019. New developments in fracture of rubbers: Predictive tools and influence of thermal aging. Int. J. Solids Struct. 165, 127–136.
Naït-Abdelaziz, M., Zaïri, F., Qu, Z., Hamdi, A., Aït Hocine, N., 2012. J Integral as a fracture criterion of rubber-like materials using the intrinsic defect concept. Mech. Mater. 53, 80–90.
Planes, Emilie. 2008. 'Influence des charges sur l'évolution des propriétés mécaniques des EPDM chargés lors de leur vieillissement par irradiation'. Matériaux. Institut National des Sciences Appliquées de Lyon. http://www.theses.fr/2008ISAL0089.
Planes, E., Chazeau, L., Vigier, G., Fournier, J., Stevenson-Royaud, I., 2010a. Influence of fillers on mechanical properties of ATH Filled EPDM during ageing by gamma irradiation. Polym. Degrad. Stab. 95 (6), 1029–1038.
Planes, E., Chazeau, L., Vigier, G., Fournier, J., 2009. Evolution of EPDM networks aged by gamma irradiation – Consequences on the mechanical properties. Polymer 50 (16), 4028–4038.
Planes, E., Chazeau, L., Vigier, G., Stuhldreier, T., 2010b. Influence of silica fillers on the ageing by gamma radiation of EDPM nanocomposites. Compos. Sci. Technol. 70 (10), 1530–1536.
Pubellier, P., 2017. Influence de Charges Micrométriques Sur Le Vieillissement de Composites à Matrice Polymère. Université Paris Est, Sciences des Matériaux https://tel.archives-ouvertes.fr/tel-01799045.
Rincon-Rubio, L.M., Fayolle, B., Audouin, L., Verdu, J., 2001. A general solution of the closed-loop kinetic scheme for the thermal oxidation of polypropylene. Polym. Degrad. Stab. 74 (1), 177–188.
Rivaton, A., Cambon, S., Gardette, J.-L., 2005a. Radiochemical ageing of EPDM elastomers. 2. Identification and quantification of chemical changes in EPDM and EPR films c-irradiated under oxygen atmosphere. Nucl. Instrum. Methods Phys. Res., Sect. B 227 (3), 343–356.
Rivaton, A., Cambon, S., Gardette, J.-L., 2005b. Radiochemical ageing of EPDM elastomers. 3. Mechanism of radiooxidation. Nucl. Instrum. Methods Phys. Res., Sect. B 227 (3), 357–368.
Rosendahl, P.L., Drass, M., Felger, J., Schneider, J., Becker, W., 2019. Equivalent strain failure criterion for multiaxially loaded incompressible hyperelastic elastomers. Int. J. Solids Struct. 166, 32–46.
Seibert, D.J., Schöche, N., 2000. Direct comparison of some recent rubber elasticity models. Rubber Chem. Technol. 73 (2), 366–384.
Shabani, A., 2013. Thermal and radiochemical aging of neat and ATH Filled EPDM: Establishment of Structure/property relationships. École Nationale Supérieure d'Arts et Métiers, Mécanique-Matériaux https://pastel.archives-ouvertes.fr/pastel-00941289.
Sidi, A., 2016. Etude de la dégradation radiolytique de polymères constitutifs de câbles contrôle/commande K1 en ambiance nucléaire. Chimie-Physique. Université Blaise Pascal https://tel.archives-ouvertes.fr/tel-01593262.
Tobolsky, A.V., Metz, D.J., Mesrobian, R.B., 1950. Low temperature autoxidation of hydrocarbons: the phenomenon of maximum rates 1,2. J. Am. Chem. Soc. 72 (5), 1942–1952.
Trapper, P., Volokh, K.Y., 2010. Modeling dynamic failure in rubber. Int. J. Fract. 162 (1-2), 245–253.
Valentín, J.L., Carretero-González, J., Mora-Barrantes, I., Chassé, W., Saalwächter, K., 2008. Uncertainties in the determination of cross-link density by equilibrium swelling experiments in natural rubber. Macromolecules 41 (13), 4717–4729.
Visakh, P.M., Thomas, S. (Eds.), 2013. Advances in elastomers. 2: Composites and nanocomposites. Springer, Berlin.
Volokh, K., 2007. Hyperelasticity with softening for modeling materials failure. J. Mech. Phys. Solids 55 (10), 2237–2264.
Volokh, K.Y., 2013. Review of the energy limiters approach to modeling failure of rubber. Rubber Chem. Technol. 86 (3), 470–487.
Volokh, K.Y., 2010. On modeling failure of rubber-like materials. Mech. Res. Commun. 37 (8), 684–689.
Volokh, K.Y., 2017. Loss of ellipticity in elasticity with energy limiters. Eur. J. Mech. A. Solids 63, 36–42.
Wall, F.T., Flory, P.J., 1951. Statistical thermodynamics of rubber elasticity. J. Chem. Phys. 19 (12), 1435–1439.
Woo, C.S., Park, H.S., 2011. Useful lifetime prediction of rubber component. Eng. Fail. Anal. 18 (7), 1645–1651.
Zhong, D., Xiang, Y., Yin, T., Yu, H., Qu, S., Yang, W., 2019. A physically-based damage model for soft elastomeric materials with anisotropic Mullins effect. Int. J. Solids Struct. 176-177, 121–134.